

Active Sites of the Methane Dehydroaromatization Catalyst W-ZSM-5: An HRTEM Study

V. V. Kozlov^a, V. I. Zaikovskii^b, A. V. Vosmerikov^a, L. L. Korobitsyna^a, and G. V. Echevskii^b

^a Institute of Petroleum Chemistry, Siberian Branch, Russian Academy of Sciences, Tomsk, 634021 Russia

^b Boreskov Institute of Catalysis, Siberian Branch, Russian Academy of Sciences, Novosibirsk, 630090 Russia

e-mail: pika@ipc.tsc.ru

Received December 7, 2006

Abstract—Nonoxidative methane conversion into aromatic hydrocarbons on a zeolite modified with nanosized tungsten powder has been studied. The highest methane conversion and the maximum yield of aromatic hydrocarbons are attained on the catalyst containing 8.0 wt % W. The nature and the distribution of the active phases in the W-containing zeolite were investigated by high resolution transmission electron microscopy and energy dispersive x-ray spectroscopy. The deactivation of the W-HZSM-5 catalyst was studied at different stages of methane conversion. The distribution of coke deposits on the surface of the W-HZSM-5 catalyst was determined.

DOI: 10.1134/S0023158408010138

INTRODUCTION

Nonoxidative methane conversion into aromatic hydrocarbons is of great interest as an efficient method of utilization of natural and casing-head gases. In recent years, there have been publications demonstrating that high-silica zeolites modified with transition metal ions are efficient catalysts for methane dehydroaromatization (DHA) [1–5]. It is known that this reaction has two rate-limiting steps, namely, methane activation and cyclization [6–9]. It is believed that the former involves Mo-containing active sites. The aromatization step (the result of dehydrocyclization of intermediates) occurs on acid sites of the zeolite [7, 8]. An important problem is that of the stability of these catalysts, which is reduced by the carbonization of their active sites. The properties of the Mo–HZSM-5 system have been studied in greatest detail, while W-containing zeolite catalysts, which are thermally more stable [10], have received much less attention. There is almost no information about the nature of their active sites and the causes and mechanism of their deactivation.

In order to gain such information, we investigated a W–HZSM-5 catalyst at different deactivation stages during nonoxidative methane conversion into aromatic hydrocarbons by high resolution transmission electron microscopy (HRTEM) and energy dispersive X-ray (EDX) spectroscopy.

EXPERIMENTAL

Catalysts for nonoxidative methane conversion were prepared by dry mechanical mixing of high-silica ZSM-5 zeolite ($\text{SiO}_2/\text{Al}_2\text{O}_3$ molar ratio of 40) with nanosized tungsten powder (NSP) obtained by the elec-

troexplosion of a wire in argon [11]. The preparation of metal nanoparticles by electroexplosion followed by their supporting on the zeolite surface allows one to prevent the appearance of undesirable impurities typical of conventional impregnation syntheses (Cl, S, N, etc.). The tungsten NSP content of the catalyst was varied between 3.0 and 10.0 wt %. The mixing of initial samples was carried out in a KM-1 jar mill (East Germany) in air for 4 h. The resulting mixture was calcined at 550°C for 5 h, pressed into pellets, and ground. The 0.5–1.0 mm size fraction was used in our study.

Catalysts were tested in a flow apparatus. A sample (0.6 g) was placed onto the quartz grid of a quartz reactor (12 mm in diameter), heated to 750°C in helium, and kept at this temperature for 20 min. Next, the catalyst was treated with methane (99.9%) under the following conditions: reaction temperature, 750°C; methane GHSV, 1000 h^{-1} ; low overpressure. The reaction products were analyzed by gas chromatography at 40-min intervals.

The morphology and distribution of active phases in the zeolite support and the formation and nature of carbon deposits were studied by HRTEM. To do this, we sampled the catalyst that showed the highest activity in methane dehydroaromatization (8.0% W–HZSM-5) after 10-, 60-, and 420-min-long operation.

HRTEM examinations were carried out on a JEM-2010 electron microscope (JEOL, Japan) at an accelerating voltage of 200 kV and a linear resolution of 0.14 nm. In the local elemental analysis of catalysts, we used an EDAX (EDAX Co.) energy-dispersive X-ray spectrometer coupled with the electron microscope. The spectrometer was fitted with a Si(Li) detector with a resolution of at least ≥ 130 eV. The minimum diameter

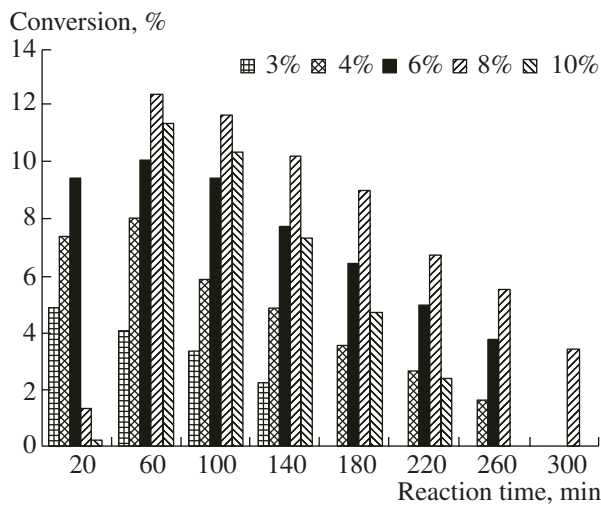


Fig. 1. Change of methane conversion in the course of the reaction on W-HZSM-5 catalysts containing different amounts of tungsten.

of the electron probe corresponding to the limiting spatial locality of elemental analysis was 10 nm. The samples for electron microscopic analysis were mounted on holey carbon substrates fixed on copper grids.

RESULTS AND DISCUSSION

The investigation of methane conversion at 750°C and a GHSV of 1000 h⁻¹ showed that aromatic hydrocarbons, mainly, benzene, toluene, and naphthalene, form in the presence of the W-HZSM-5 catalysts. Figure 1 shows how the methane conversion depends on the concentration of the tungsten nanopowder added to the zeolite. The most efficient catalyst for methane DHA contains 8.0 wt % W; the maximum catalytic activity is attained after 60-min-long operation. Detailed information about the catalytic properties of W-ZSM-5 samples in nonoxidative methane conversion is reported in [12].

From the electron micrographs, it is seen that, before the reaction, the calcined samples have large particles (several tens of nanometers in size) on the zeolite surface. According to electron microdiffraction data, these particles are the WO₃ phase. The ionic form of oxidized tungsten is distributed over the surface of the zeolite. This was also observed by HRTEM and EDX spectroscopy.

By these methods, it was found that the initial stage of the reaction on the 8.0% W-HZSM-5 catalyst yields tungsten carbide. This carbide is stabilized in two forms. The first form is observed on the surface of the zeolite as particles 5–20 nm in size (Fig. 2a). Using the electron microdiffraction method and the Fourier analysis of HRTEM images obtained by direct imaging of the crystal lattice, this phase was identified as α -W₂C (Fig. 2b) [13]. On the catalyst surface, there are also

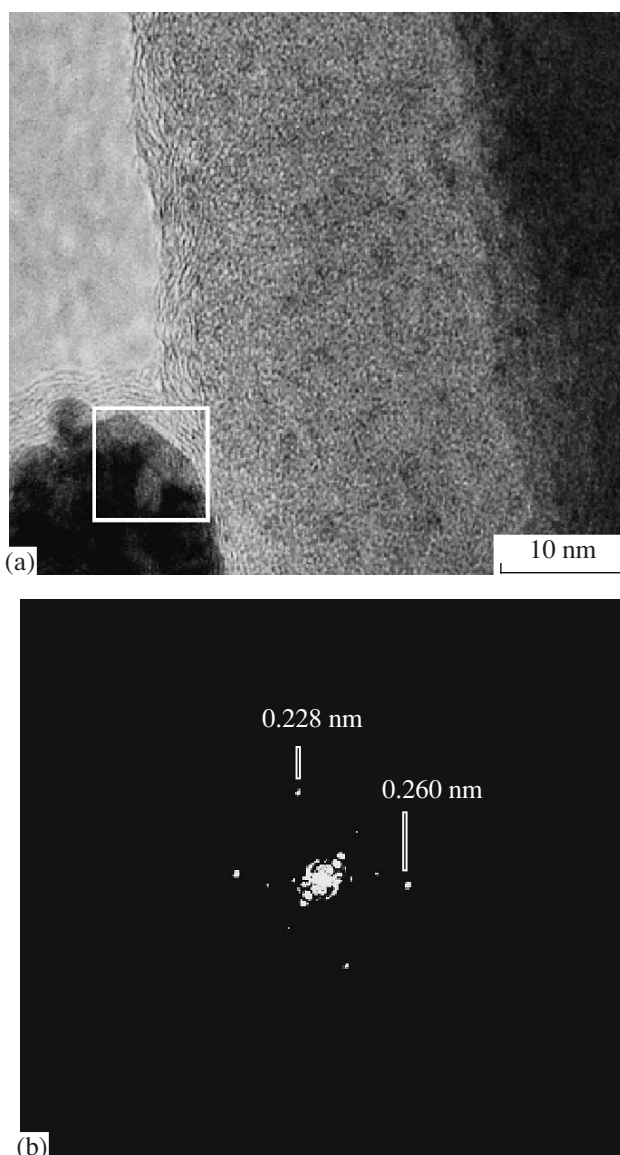


Fig. 2. HRTEM image of an area of the catalyst surface: (a) crystal lattice of tungsten carbide and (b) halftone image of the two-dimensional Fourier transform of this area.

large particles of α -W₂C up to 100 nm in size, which apparently result from the agglomeration of smaller particles. Tungsten oxide particles were not found on the zeolite surface.

Besides a coarser form of tungsten oxide, a fine fraction as particles 1 nm in size was observed by the HRTEM method in the samples that had been on stream for 60 and 420 min. These particles are arranged in inner zeolite channels. The EDX spectra from zeolite areas containing fine fractions, but without surface particles of tungsten carbide, show a signal from W. This proves the presence of W-containing clusters in the bulk of the zeolite. It should be noted that, according to HRTEM data, there are no such clusters on the zeolite surface. The appearance of the clusters localized in zeo-

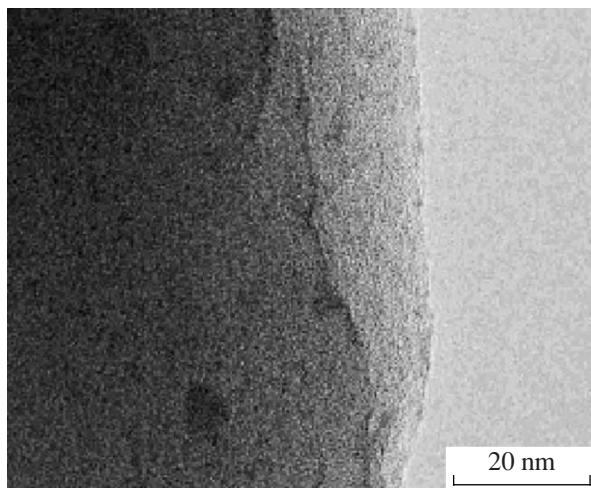


Fig. 3. Micrograph of an edge of a zeolite particle that had been on stream for 10 min.

lite channels and of large particles of tungsten carbide on the zeolite surface testifies to the redistribution of tungsten in the catalyst during methane DHA. Tungsten-containing sites formed in the inner channels and on the zeolite surface are of very different natures. The longer the catalyst operates, the larger the number of clusters inside the channels. Furthermore, tungsten carbide aggregates on the surface to give a large number of sufficiently massive particles (Figs. 3–6). It was determined earlier that the activity of the Mo–HZSM-5 catalyst may decrease due to zeolite dealumination as a result of the formation of molybdenum aluminates [14, 15]. The EDX examination of the W–HZSM-5 catalyst that had been on stream for 60 min showed that aluminum and silicon ions are not present in the massive particles on the zeolite surface. The X-ray spectrum consists of only two lines—tungsten and carbon ones; therefore, this particle is tungsten carbide (Fig. 5c). We may conclude that during the maximum catalytic activ-

ity period, zeolite dealumination and the formation of tungsten aluminates do not occur.

It is obvious that, under conditions of methane activation in the course of the reaction, the active catalytic sites may be subjected to coking to an extent depending on the conversion of methane into intermediates. A fragment of the W-modified zeolite catalyst after 10 min of reaction is shown in Fig. 3. By this time, a carbon layer with graphite-like structure, 2–4 nm in thickness, forms on the particles of tungsten carbide on the surface of the catalyst (Fig. 4). Otherwise, there are no carbonic deposits on the zeolite surface. Only after a 60-min-long reaction do graphite-like deposits 1–2 nm in thickness begin to form on the outer zeolite surface. These deposits have “island” morphology; however, most of the support remains uncoked. At the same time, the coke layer thickness on the tungsten carbide surface is 3–5 nm (Figs. 5a, 5b). The coke has a graphite-like structure: from the electron micrographs, it is seen that the atomic graphite layers are arranged periodically, separated by a distance of 0.35 nm. This value is close to the interplanar spacing d_{002} of the graphite phase.

As on the Mo–HZSM-5 catalyst [14, 15], on the W–HZSM-5 the graphite layer thickness on the tungsten carbide particles practically does not change as the reaction time is extended to 60 and even 420 min (Figs. 5a, 6). This shows that W_2C particles participate in methane activation followed by its partial decomposition, but only at the initial reaction stage. After the formation of a sufficiently dense coating on the surface of these particles due to graphite-like deposits, the deactivation of active sites on the surfaces of large particles of tungsten carbide occurs. This happens after 10 min of the reaction. In spite of this, the catalyst retains a high activity afterwards. It appears from this that the principal role in methane activation on the catalyst is played by the W-containing clusters in the inner zeolite channels. Considering the conditions of carbon-forming methane conversion, and also the interaction

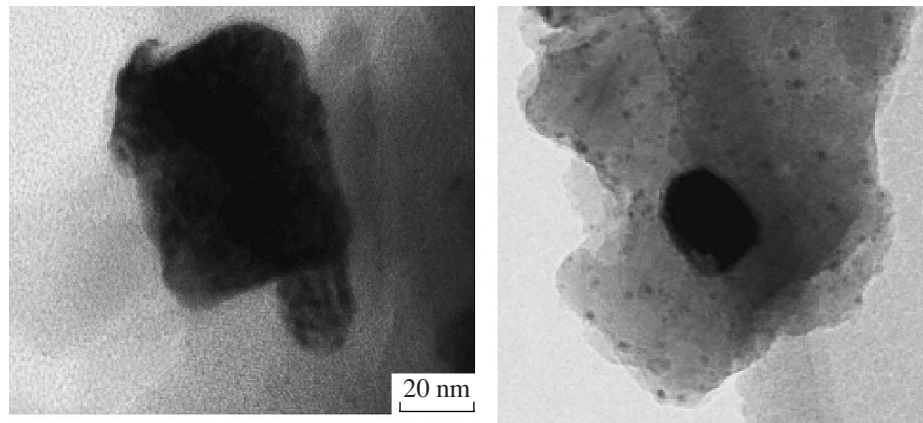


Fig. 4. Micrographs of the particles of tungsten carbide on the zeolite surface that had been on stream for 10 min.

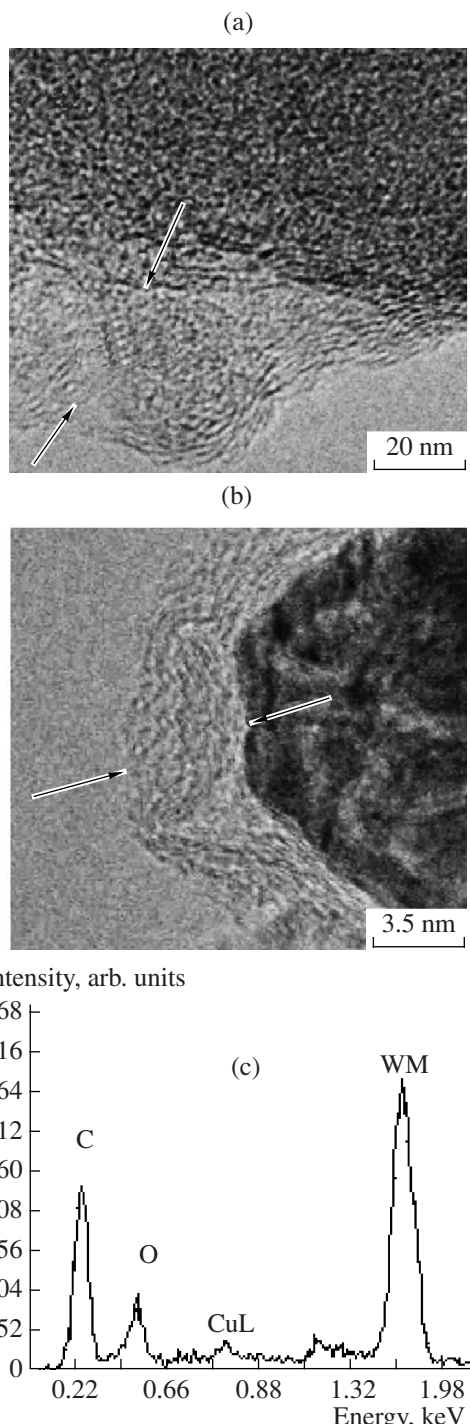


Fig. 5. Micrographs of (a) the coked zeolite surface and (b) a particle of tungsten carbide that had been on stream for 60 min. (c) EDX spectrum of the tungsten carbide particle.

between tungsten and oxygen in the zeolite channels, we can assume that the clusters consist of fine oxidized particles of tungsten carbide $W(C, O)$. (Examples of oxidized particles of tungsten carbide are reported in [13].) The high-resolution electron micrographs indicated the accessibility of the zeolite surface and chan-

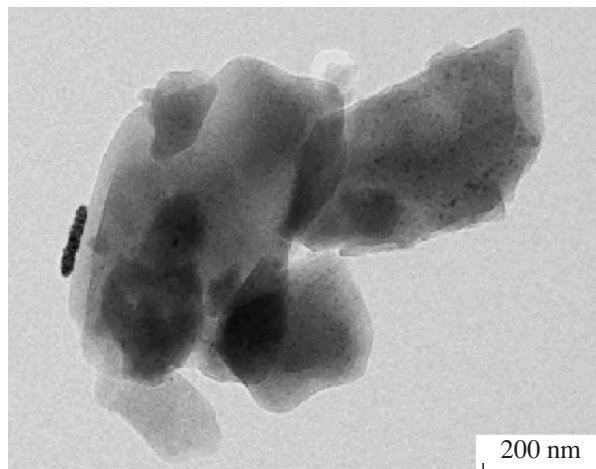


Fig. 6. Micrograph of tungsten clusters in the bulk of the zeolite and particles of tungsten carbide on the zeolite surface after a 420-min-long reaction.

nels to methane molecules throughout the reaction involving the W-HZSM-5 catalyst. During this time zeolite is slightly subjected to coking, and only small “islands” of carbon with a graphite-like structure form.

We may conclude that, after methane activation on W-containing cluster sites, dimerization and transformation of DHA intermediates may occur on Brønsted sites [7, 8] inside the holes and on zeolite surface. The formation of cokes on these cluster centers occurs much more slowly than on the surface of particles of the W_2C phase. This ensures a higher stability of the W-HZSM-5 catalyst in methane dehydroaromatization.

REFERENCES

1. Wang, L., Tao, L., Xie, M., Xu, G., Huang, J., and Xu, Y., *Catal. Lett.*, 1993, vol. 21, p. 35.
2. Weckhuysen, W.N., Wang, D., Rosynek, M.P., and Lunsford, Y.H., *J. Catal.*, 1998, vol. 175, p. 338.
3. Shuang Li, Chunlei Zhang, and Qiebin Kan, *Appl. Catal.*, 1999, vol. 187, p. 199.
4. Vosmerikov, A.V., Echevsky, G.V., Korobitsyna, L.L., Arbuzova, N.V., Velichkina, L.M., Zhuravkov, S.P., Barbashin, Ya.E., and Kodenev, E.G., *Eurasian Chem. Tech. J.*, 2004, vol. 6, no. 3, p. 201.
5. Vosmerikov, A.V., Echevskii, G.V., Korobitsyna, L.L., Barbashin, Ya.E., Arbuzova, N.V., Kodenev, E.G., and Zhuravkov, S.P., *Kinet. Katal.*, 2005, vol. 46, no. 5, p. 769 [*Kinet. Catal. (Engl. Transl.)*, vol. 46, no. 5, p. 724].
6. Chen, L., Lin, L., and Xu, Z., *J. Catal.*, 1995, vol. 167, no. 2, p. 190.
7. Wang, L., Xu, Y., and Wang, S., *J. Catal.*, 1997, vol. 169, no. 1, p. 11.
8. Wang, D., Lunsford, J.H., and Posynek, M.P., *J. Catal.*, 1997, vol. 169, no. 1, p. 347.
9. Pierella, L.B. and Wang, L., *Kinet. Catal. Lett.*, 1997, vol. 60, p. 101.

10. Jin-Long Zeng, Zhi-Tao Xiong, Hong-Bin Zhang., Guo-Dong Lin, and Tsai, K.R., *Catal. Lett.*, 1998, vol. 53, p. 119.
11. Kotov, Yu.A. and Yavorovskii, N.A., *Fiz. Khim. Obrab. Mater.*, 1978, no. 4, p. 24.
12. Vosmerikov, A.V., Echevskii, G.V., Korobitsyna, L.L., Arbuzova, N.V., Kodenev, E.G., Velichkina, L.M., and Zhuravkov, S.P., *Kinet. Katal.*, 2007, vol. 48, no. 3, p. 432 [*Kinet. Catal.* (Engl. Transl.), vol. 48, no. 3, p. 409].
13. *Powder Diffraction File 2*, Swarthmore, Pa.: Joint Committee on Powder Diffraction Standards, 1997, nos. 40-0752, 22-0959.
14. Zaikovskii, V.I., Vosmerikov, A.V., Anufrienko, V.F., Korobitsyna, L.L., Kodenev, E.G., Echevskii, G.V., Vassenin, N.T., Zhuravkov, S.P., Ismagilov, Z.R., and Parmon, V.N., *Dokl. Akad. Nauk*, 2005, vol. 404, no. 4, p. 500 [*Dokl. Phys. Chem.* (Engl. Transl.), vol. 404, part 2, p. 201].
15. Zaikovskii, V.I., Vosmerikov, A.V., Anufrienko, V.F., Korobitsyna, L.L., Kodenev, E.G., Echevskii, G.V., Vassenin, N.T., Zhuravkov, S.P., Matus, E.V., Ismagilov, Z.R., and Parmon, V.N., *Kinet. Katal.*, 2006, vol. 47, no. 3, p. 396 [*Kinet. Catal.* (Engl. Transl.), vol. 47, no. 3, p. 389].